

AperTO - Archivio Istituzionale Open Access dell'Università di Torino

**Fatigue of self-healing hierarchical soft nanomaterials: The case study of the tendon in sportsmen**

**This is the author's manuscript**

*Original Citation:*

*Availability:*

This version is available <http://hdl.handle.net/2318/151106> since 2016-10-31T23:32:28Z

*Published version:*

DOI:10.1557/jmr.2014.335

*Terms of use:*

Open Access

Anyone can freely access the full text of works made available as "Open Access". Works made available under a Creative Commons license can be used according to the terms and conditions of said license. Use of all other works requires consent of the right holder (author or publisher) if not exempted from copyright protection by the applicable law.

(Article begins on next page)



# UNIVERSITÀ DEGLI STUDI DI TORINO

***This is an author version of the contribution published on:***

*Questa è la versione dell'autore dell'opera:*

*[Journal of Materials Research 30(1), 2014, DOI: 10.1557/jmr.2014.335]*

***The final version is available at:***

*La versione definitiva è disponibile alla URL:*

*[<http://journals.cambridge.org/action/displayAbstract?fromPage=online&aid=9475231&fileId=S0884291414003355>]*

**Fatigue of self-healing hierarchical soft nanomaterials:  
the case study of the tendon in sportsmen**

Federico Bosia<sup>(1)</sup>, Matthew Merlino<sup>(2)</sup> and Nicola M. Pugno<sup>(3,4,5)\*</sup>

(1) *Department of Physics and “Nanostructured Interfaces and Surfaces”  
Interdepartmental Centre, Università di Torino, Via P. Giuria 1, 10125, Torino, Italy.*

(2) *Department of Electrical Engineering & Computer Science, Massachusetts Institute  
of Technology, 77 Massachusetts Ave, Cambridge, MA 02139, United States.*

(3) *Laboratory of Bio-Inspired & Graphene Nanomechanics, Department of Civil,  
Environmental and Mechanical Engineering, Università di Trento, via Mesiano, 77, I-38123  
Trento, Italy.*

(4) *Center for Materials and Microsystems, Fondazione Bruno Kessler, Via Sommarive  
18, I-38123 Povo (Trento), Italy.*

(5) *School of Engineering and Materials Science, Queen Mary University of London,  
Mile End Road, London E1 4NS.*

(\* Corresponding author: [nicola.pugno@unitn.it](mailto:nicola.pugno@unitn.it)

**Abstract:** One of the defining properties of biological structural materials is that of self-healing, i.e. the ability to undergo long-term reparation after instantaneous damaging events, but also after microdamage due to repeated load cycling. To correctly model the fatigue life of such materials, self-healing must be included in fracture and fatigue laws and related codes. Here, we adopt a numerical modelization of fatigue cycling of self-healing biological materials based on the Hierarchical Fibre Bundle Model and propose modifications in Griffith's and Paris' laws to account for the presence of self-healing. Simulations allow to numerically verify these modified expressions and highlight the effect of the self-healing rate, in particular for collagen-based materials such as human tendons and ligaments. The study highlights the robustness of the self-healing strategy adopted in Nature, and provides the possibility of improving the reliability of predictions on fatigue life in sports medicine.

**Keywords:** Self-healing, Fatigue, Fracture, Tendon, Simulations.

## 1. Introduction

One of the distinctive characteristics of biological structural materials is their ability to autonomically repair progressive damage, or in other words to achieve self-healing<sup>1,2</sup>. Typical examples are skin, bone or tendons, where the long term reparation occurs as a result of initial or damaging event<sup>3</sup>. Drawing inspiration from these natural systems, self-healing artificial materials have also been designed and produced, using diverse approaches and various constituents, from systems based on “microcapsules” containing a healing agent<sup>4, 5</sup>, to “vascular-based” systems<sup>6, 7</sup>, to “molecular-based” systems<sup>8, 9</sup>. In particular, self-healing was found to be particularly effective in increasing fatigue life of composites<sup>10, 11</sup> and polymers<sup>12</sup>, where up to 90% recovery of fracture toughness was achieved. A review of approaches to self-healing in artificial materials can be found in<sup>13</sup>, while a review of numerical modelling methods applied to such systems is given in<sup>14</sup>.

In biological materials, damage generally evolves as a consequence of cyclic loading during the whole lifetime of a particular tissue. Tendons and ligaments are typical examples. Their function is to transmit forces between bones and muscles or bones and other bones, and are constituted essentially by type I collagen fibres<sup>1</sup>. As for other biological structural materials, they display a hierarchical structure that encompasses various size scales, ranging from collagen molecules (nanometer scale), to microfibrils, to fibrils, to fibres, to fibre fascicles, to the final tissue itself (at cm scale)<sup>15</sup>. Thus, tendons and ligaments can be considered an example of “soft nanomaterials”. From a mechanical point of view, they can be modelled as bundles of viscoelastic fibres organized in a hierarchical structure, cyclically loaded in the fibre direction in uniaxial tension. Thus, a fibre bundle model-like approach<sup>16</sup> with the inclusion of hierarchy and self-healing is ideally suited to simulate the mechanical

behaviour of these biological structures. In previous work, we introduced such a Hierarchical Fibre Bundle Model (HFBM)<sup>17, 18</sup> coupled with self-healing<sup>19</sup> to study the effects of material regeneration on the strength and toughness of hierarchical composite materials.

As mentioned above, damage to tendons and ligaments can be caused by macro-traumas but more often to repeated exposure to lower magnitude stresses, i.e. fatigue. In the case of humans, healthy individuals are estimated to walk approximately 1-1.5 million strides per year, and in sporting activities so-called “tendon overuse injuries” are estimated to be about 30-50% of all sports-related injuries<sup>20</sup>. Clearly, however, tendon inflammation, degeneration and ultimately fatigue life depends on the stress level to which they are subjected. For example, cyclic loading at a 40% level of the Ultimate Tensile Strength (UTS) would typically lead to failure after approximately 8500 cycles, whilst at 20% of the UTS, the fatigue life would be of the order of 300000 cycles (i.e. about four months of normal walking activity)<sup>21</sup>. This type of prediction however is based on results from *in vitro* mechanical tests on tendons<sup>22</sup>, whilst self-healing and remodelling effects are present *in vivo* and cannot be neglected. Thus, a numerical model which is able to estimate fatigue life of tendons starting from known mechanical properties and including self-healing effects would be of considerable interest to help e.g. in the diagnosis and prediction of overuse injuries. In this paper, we extend the above-mentioned HFBM to simulate cyclic loading and thus fatigue, and study the influence of self-healing on biological materials such as tendons and ligaments.

The paper is structured as follows: in Section 2, the theoretical influence of self-healing on fracture stress and fatigue life is discussed; in Section 3, the numerical approach is presented; in Section 4 calculation and simulation results are compared and discussed. Conclusions conclude the paper.

## 2. Fracture stress and fatigue life laws in the presence of self-healing

We wish to analytically estimate the scaling of fracture stress and fatigue life in self-healing materials as a function of their healing rate  $\eta$ . Self-healing is a function of time, but also of damage level, since it is triggered by damage, increases with damage, and stops if no further damage occurs, albeit with some time delay. Here, we consider loading to be slow enough for the system to be described in the steady-state regime, so that dependence with respect to time can be neglected, and only dependence with respect to damage level is significant. Thus, the healing rate  $\eta$ , which is a function of time and damage level, can be defined as the ratio between the “healed” volume portion of the material and the “damaged” volume portion in a given fixed time interval. As a first approximation, we will consider  $\eta$  constant.

We first consider the relation for the scaling of the fracture stress  $\sigma_F$  in an infinite linear elastic plate with central crack of length  $2a$  and subjected to uniaxial tension perpendicularly to the crack (Griffith’s case), which according to Linear Elastic Fracture Mechanics (LEFM)<sup>23</sup> is  $\sigma_F \propto K_{IC} / \sqrt{\pi a}$ , where  $K_{IC}$  is the critical stress intensity factor, or fracture toughness, for mode I crack propagation. If we now consider that the effect of self-healing is to limit crack growth, we can as a first approximation assume that the crack length term  $a$  is modified to  $a \cdot (1 - \eta)$  in the presence of self-healing, so that the fracture stress  $\sigma_F^{(SH)}$  becomes:

$$\sigma_F^{(SH)} \propto \frac{K_{IC}}{\sqrt{\pi a (1 - \eta)}} \quad (1)$$

This equation can be generalized in the case of nonlinear elastic materials, such as biological tissues like tendons or ligaments, for which the stress/strain constitutive equation can be expressed as  $\sigma \propto \varepsilon^\kappa$ , with  $\kappa$  constant ( $\kappa > 1$  implies hyperelasticity while  $\kappa < 1$  implies elastoplasticity)<sup>24</sup>. Writing the equation in the form of the ratio between fracture stresses with and without self-healing, we get:

$$\frac{\sigma_F^{(SH)}}{\sigma_F} = \left[ \frac{K_{IC}}{\sigma_F \sqrt{\pi a} (1-\eta)} \right]^{2\alpha} = \frac{K_{IC}^{(SH)}}{\sigma_F \sqrt{\pi a}} \quad (2)$$

where  $\alpha = \kappa/(\kappa+1)$  and the modified fracture toughness for self-healing materials  $K_{IC}^{(SH)}$  is:

$$K_{IC}^{(SH)} = \frac{\sigma_F^{(1-2\alpha)} (\pi a)^{\left(\frac{1}{2}-\alpha\right)} K_{IC}^{2\alpha}}{(1-\eta)^\alpha} \quad (3)$$

which means that both the fracture stress and fracture toughness of a self-healing material are expected to scale as  $\sigma_F^{(SH)} \propto K_{IC}^{(SH)} \propto (1-\eta)^{-\alpha}$  with respect to the healing rate  $\eta$ .

As far as fatigue life is concerned, one of the most widely used analytical laws is that of Paris<sup>25</sup>, which describes the growth of a fatigue crack of length  $a$  as a function of the number of cycles  $N$  between two stress levels  $\sigma_{min}$  and  $\sigma_{max}$  as  $da/dN \propto (\Delta\sigma \sqrt{\pi a})^m$  where  $\Delta\sigma = \sigma_{max} - \sigma_{min}$ . Integrating this equation, we find that the number of cycles to failure  $N_C$ , arising when the crack length has reached its critical final value  $a_C$ , scales as:



$$N_C \propto a^{(1-m/2)} \quad (4)$$

where for  $m=2$  a logarithmic expression would emerge<sup>26</sup>.

This scaling relation can once again be generalized for a self-healing material with the above hypothesis, so that:

$$N_C^{(SH)} \propto [a(1-\eta)]^{(1-m/2)} \quad (5)$$

which can again be generalized for nonlinear elastic materials, giving:

$$N_C^{(SH)} \propto \left\{ [a(1-\eta)]^{(1-m/2)} \right\}^{2\alpha} \propto (1-\eta)^{\alpha(2-m)} \quad (6)$$

### 3. Numerical Hierarchical Fibre Bundle Model for self-healing and fatigue

As mentioned in Section 1, tendons and ligaments display a fibrous structure, and several hierarchical levels can be identified<sup>27, 28</sup>, as shown in Fig. 1: from tissue level ( $\sim$  cm), to collagen fibres ( $\sim$  mm in length,  $\sim$   $\mu$ m in diameter), to collagen fibrils ( $\sim$   $\mu$ m in length,  $\sim$  100 nm in diameter), to collagen molecules ( $\sim$  300 nm in length,  $\sim$  1 nm in diameter). Therefore, as in previous studies, we simulate their mechanical behaviour using a hierarchical fibre bundle model (HFBM)<sup>18, 19</sup> which extends the classical fibre-bundle model<sup>16</sup>, adding hierarchical and self-healing effects. The HFBM procedure consists in discretizing a specimen in arrays of fibres arranged in series and parallel and assigning them statistically distributed fracture strengths, using a Weibull distribution<sup>29</sup>. Uniaxial loading is applied to the specimen

and when fibres fail due to their strength having been exceeded, the load is redistributed among parallel fibres according to an Equal Load Sharing scheme. This allows the system to be analytically solvable at each iteration, i.e. the stresses acting on each fibre can be recalculated after each fracture event, as well as the mechanical properties of each section of the bundle, and the global stress strain behaviour. The model is implemented in a MATLAB code which generates statistically-distributed random fibre strength values from the chosen Weibull distributions for each fibre type, calculates the global stress-strain data for the selected loading protocol, and repeats the simulation with different random values over a sufficient number of iterations in order to derive statistically reliable average values. For large systems, the code is run on a high-performance computing cluster at the Politecnico di Torino<sup>30</sup>.

Hierarchical architectures can be modelled by using the simulation output of one particular hierarchical level (e.g. overall strength and stiffness) as the input for the statistically-assigned mechanical properties at the next hierarchical level<sup>17</sup>. Self-healing is included in this scheme by allowing fibres to be “regenerated” (healing event) as well as “eliminated” (fracture event) at a certain healing rate  $\eta$ , which is defined as:

$$\eta = \frac{N_{sh} - N_{s0}}{N_0 - N_{s0}} \quad (7)$$

where  $N_0$  is the initial number of fibres, and  $N_{s0}$  and  $N_{sh}$  are the numbers of surviving fibres with or without self-healing<sup>19</sup>, respectively. If  $N_h$  or  $N_f$  are the number of healed or fractured fibres, respectively, in a given time interval, we have  $N_{sh} = N_0 - N_f + N_h$  and  $N_{s0} = N_0 - N_f$ , so that:

$$\eta = \frac{N_h}{N_f} \quad (8)$$

in accordance with the definition given in Section 2. Finally, self-healing can take place at random locations in the specimen (distributed healing, in the case of microcracking) or at the location of the main advancing cracks (localized healing).

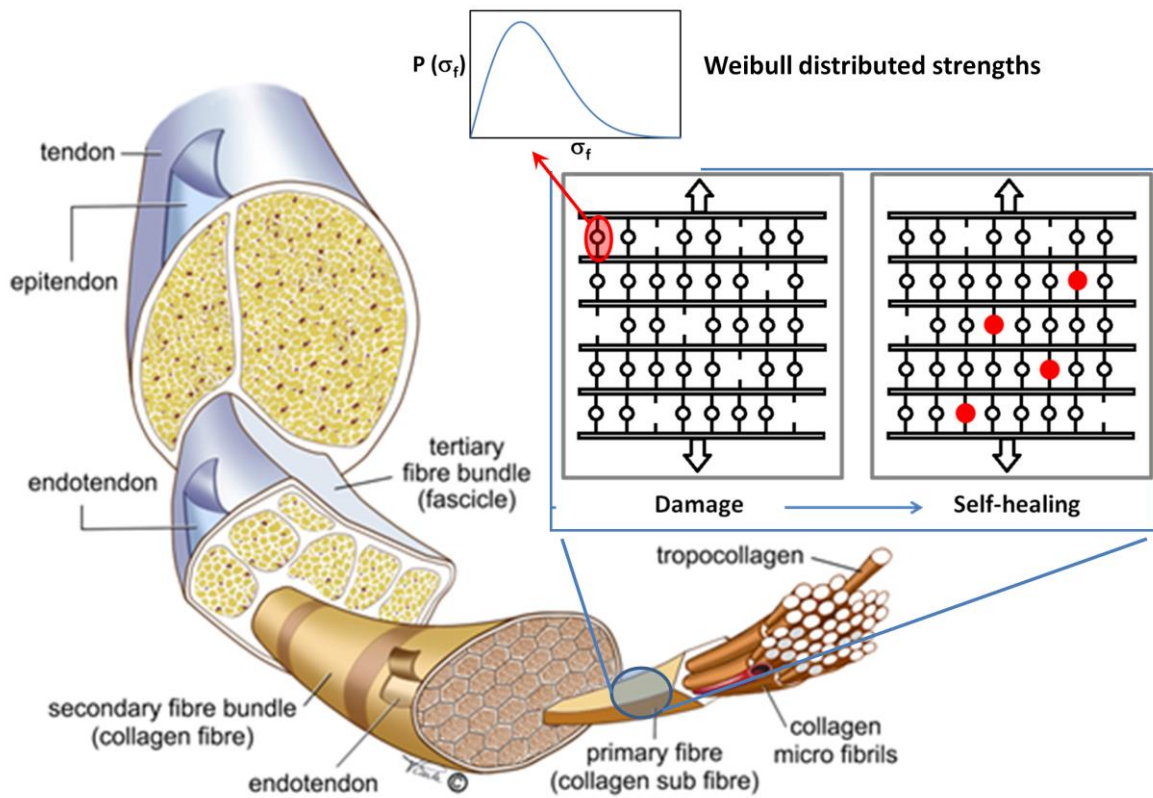


Figure 1: Hierarchical fibrous structure of tendon, from tissue level to collagen fibre bundles, down to collagen fibrils (printed with permission of Vicky Earle and Karim Khan and not to be reproduced further), and a schematic of the corresponding HFBM modelization including self-healing.

In the case of fatigue damage progression, modifications are necessary to the numerical model with respect to simulations involving simple monotonically increasing loads. This is due to the previously discussed Paris' law, which predicts a decrease of fatigue strength  $\sigma_C$  with increasing number of cycles:

$$\sigma_C \propto N_C^{1/(1-m/2)} \quad (9)$$

where  $N_C$  is the number of cycles to failure. The typical behaviour is shown in Fig. (2) for  $m = 5$  and various values of initial crack length  $a$ . Here, fatigue strength is normalized with respect to nominal fracture strength.

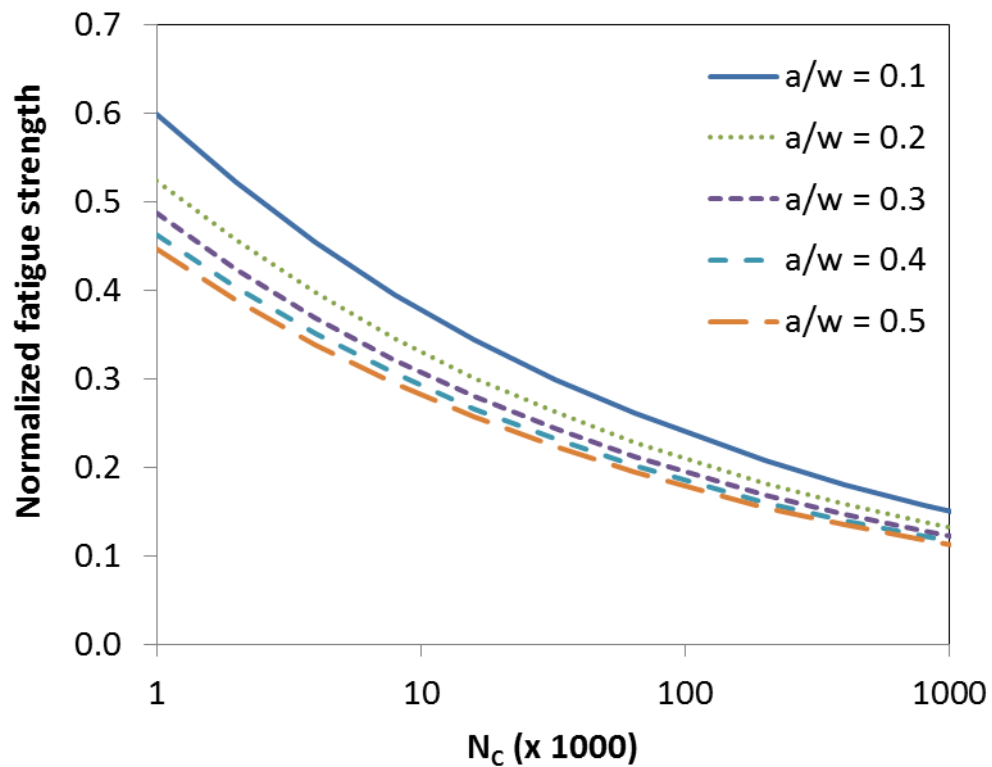


Figure 2: Fatigue strength decrease with increasing number of cycles  $N_C$ , for various initial

*crack lengths  $a$  with respect to the specimen width  $w$  ( $m=3$ ). Fatigue strength is normalized with respect to nominal fracture strength.*

Therefore, the failure criterion for the individual fibres in the HFBM is modified in order to include a stress threshold, whose initial value is assigned according to a Weibull distribution, which decreases with the number of fatigue cycles, according to Eq. (9).

When simulating biological materials, where the healed tissue is the same as the original one, the mechanical characteristics of the “healing agent” are the same as those of the “host material”. This means that when healing occurs, fractured fibres in the bundle are replaced by fibres with statistically equivalent mechanical characteristics. To model tendons or ligaments, we use representative mechanical properties<sup>20-22</sup>: Young’s modulus  $E = 650$  MPa, Failure stress  $\sigma_F = 80$  MPa, failure strain  $\varepsilon_F = 15\%$ . Weibull distributions with shape parameter  $k=2$  are used to obtain statistical dispersion around these mean values.

## **4. Numerical results and analytical comparison**

### *4.1 Fracture*

We first wish to evaluate the validity of Eqs. (1-2) regarding the scaling of the strength of a self-healing material with its healing rate. To do this, we consider a specimen with a centrally placed pre-existing crack of length  $2a$ , loaded uniaxially in the direction of the fibres and perpendicular to the crack. To simulate such a pre-existing crack, an appropriate number of fibres in a central section of the fibre bundle are removed. The crack length  $a$  varies between  $1/100^{\text{th}}$  to  $1/10^{\text{th}}$  of the specimen width  $w$ , i.e. from 1% to 10% of the fibres are initially removed from the central section of the fibre bundle. Numerical simulations agree well with analytical values calculated with Eq. (2) in a wide range of parameters. As predicted by the

theory, failure stress increases with respect to  $a$  and  $(1-\eta)$  according to the power law in Eq.(2). Results shown in Fig. 3, where failure stress is normalized with respect to nominal strength  $\sigma_0$  without self-healing, refer to  $a/w = 1/50$  and a best fit is obtained for  $\alpha = 0.7$ , corresponding to  $\kappa = 2.33$ , which is close to the hypothesized value of  $\alpha = 0.5$  in the simulations. The discrepancy is due to the statistical nature of the simulations, which results in approximate scaling relations. These simulations confirm the validity of this simple scaling and thus that, in the presence of self-healing, a Griffith's crack can be treated with an equivalent length of  $a \cdot (1-\eta)$ . The obtained values for  $\alpha$  (and  $\kappa$ ) can be considered material constants, and will be used in the following sections.

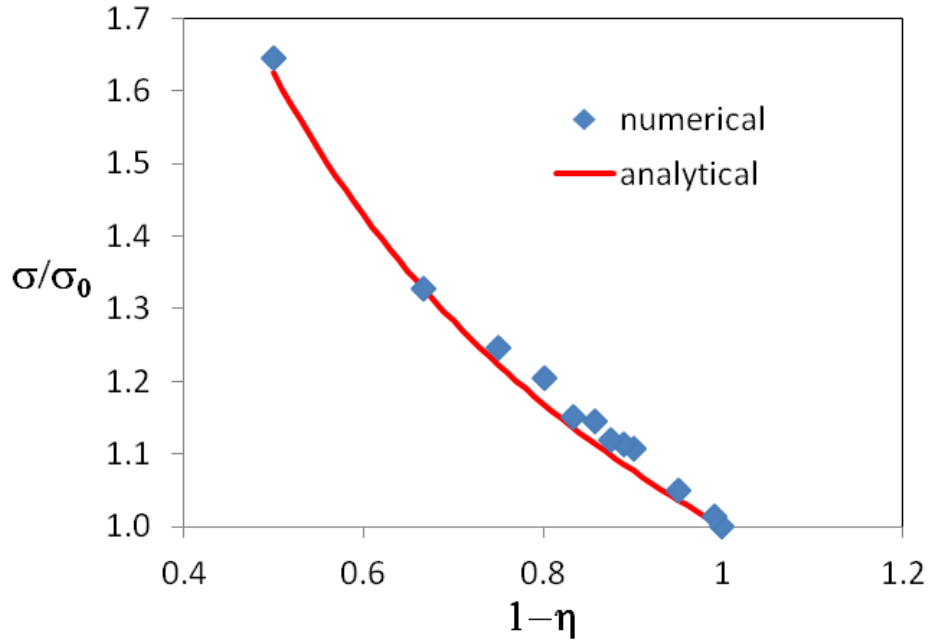


*Figure 3: Comparison between numerical simulations and analytical values based on Eq. (2) (Griffith's law generalized to include self-healing) for the failure stress  $\sigma$  of a centrally-cracked specimen as a function of its healing rate. Failure stress is normalized with respect to nominal strength  $\sigma_0$  without self-healing, and best fit is obtained for  $\alpha = 0.7$*

## *4.2 Fatigue*

The same type of sample considered in simulations in Section 4.1 is subsequently considered under cyclic fatigue loading. Various types of imposed displacement are adopted, including “saw tooth”-like functions, where the strain is increased linearly up to a maximum value, then decreased to zero, and then ramped-up again cyclically, or “rectified sine”-like functions, where the imposed strain varies with the absolute value of a sine function. An example of the obtained behaviour, in the absence of self-healing, is shown in Fig. 4a for a saw tooth cyclic strain profile. Both stresses and strains are normalized with respect to their maximum amplitude  $\varepsilon_0$  and  $\sigma_0$  in the fatigue cycles. Here, the maximum imposed strain value is chosen near the failure strain of the material (80% of the value), so that considerable damage progression is achieved over a limited number of cycles. This is visible in Fig.4b, where the stress amplitude is seen to drop considerably over few fatigue cycles, due to specimen damage, and in Fig. 4c where the specimen stress-strain curves display increasing material softening as damage progresses, up to final specimen failure.

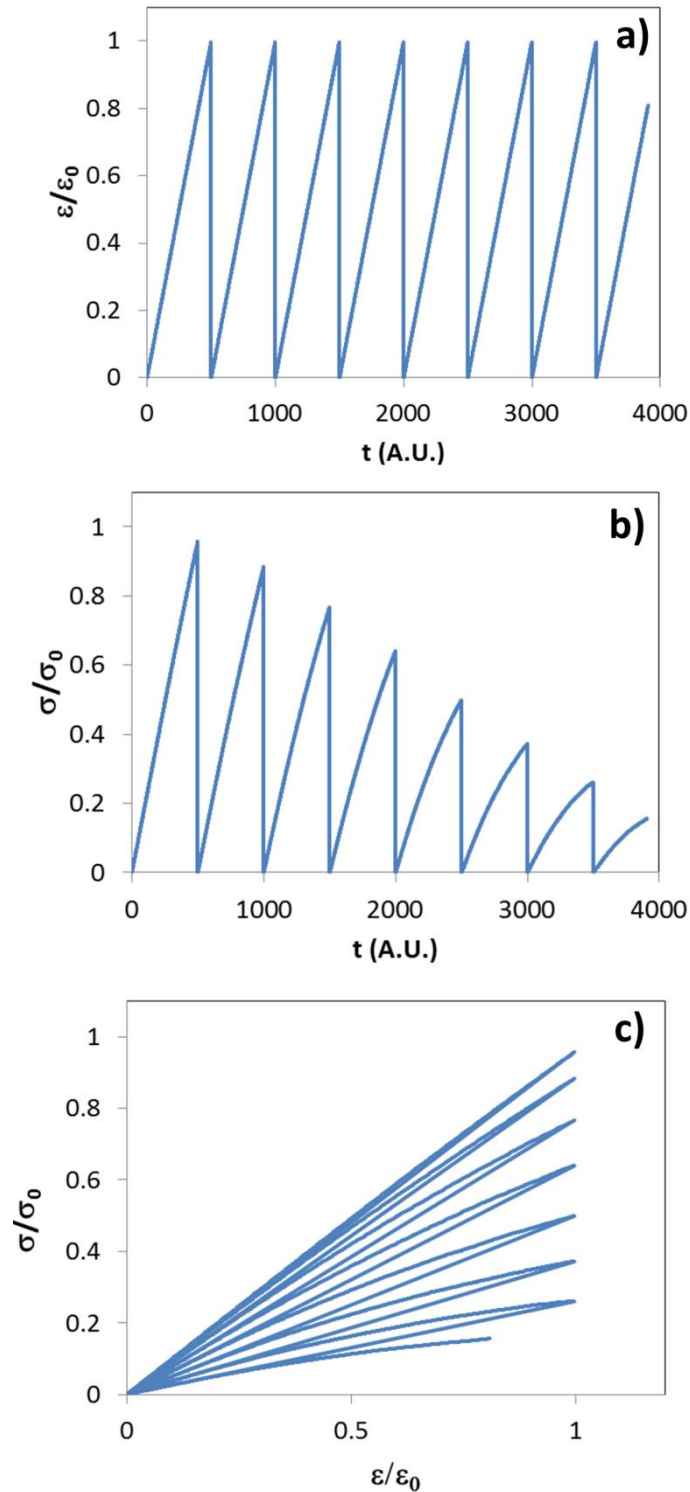


Figure 4: Example of a simulation of fatigue cycling and corresponding stress-strain behaviour: a) Cyclic "saw tooth" imposed strain; b) Corresponding stress evolution; c) resulting stress-strain curves with increasing fatigue damage. Time scales are given in



*arbitrary units (A.U.) since no explicit time dependence is included in the model.*

The effect of self-healing in the simulated behaviour can be visualized in Fig. 5 for  $\eta = 0.1$  in a distributed healing configuration: the stress softening effect due to progressive damage is reduced considerably (Fig. 5a), in particular for early stages of damage, and the fatigue lifetime is increased by approximately 34%. At the same time, the dissipated energy during fatigue cycling, calculated as the area included between the ascending and descending stress-strain curves in a single cycle, is reduced considerably in the presence of self-healing (approximately 47% per cycle, Fig. 5b). Clearly, this calculation does not account for the energy necessary to provide self-healing itself. At specimen failure, the self-healing specimen dissipates a greater amount of total energy, since it fails at a higher stress value with respect to the non-self-healing one.

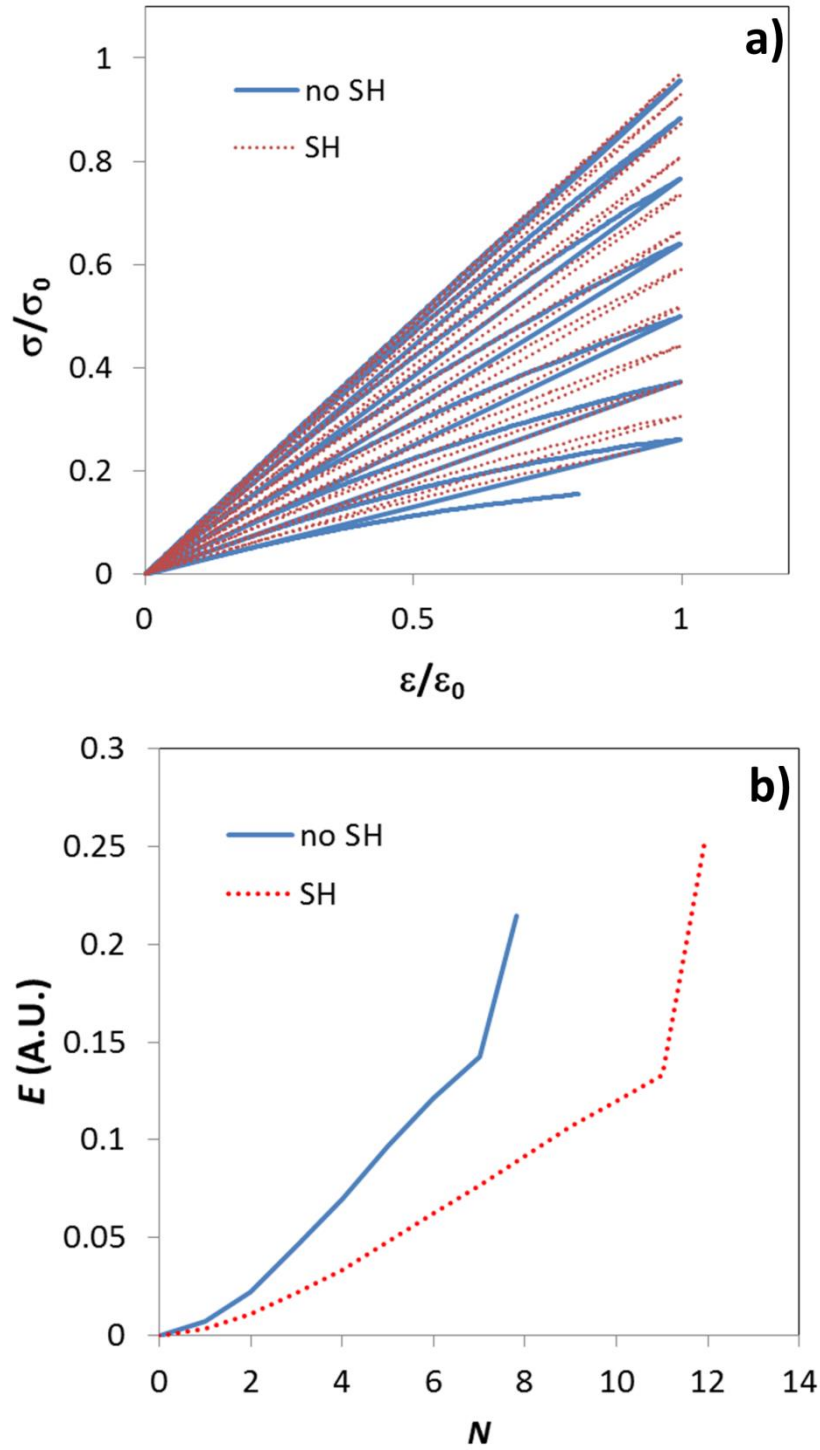
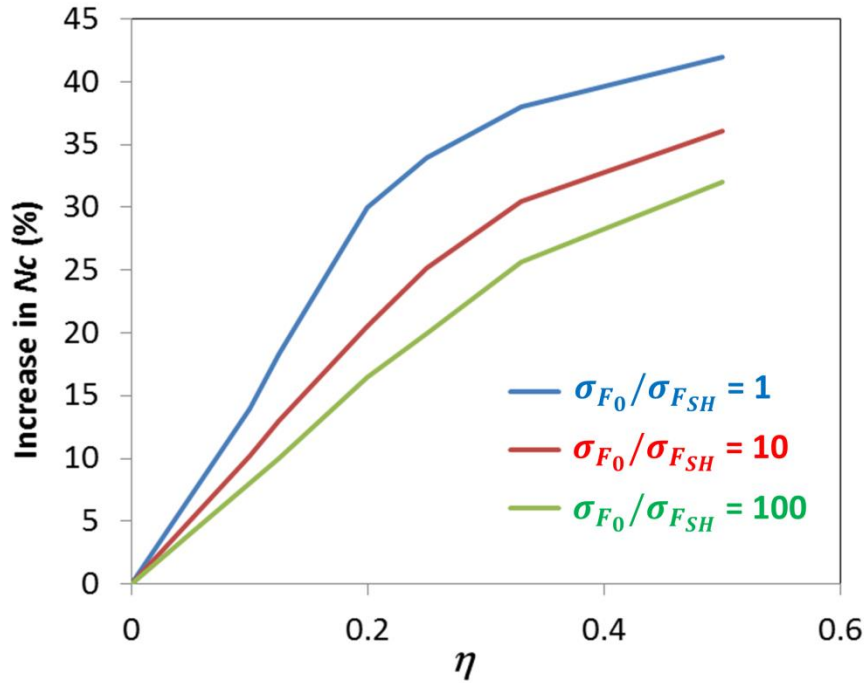


Figure 5: Example of a simulation of fatigue cycling with (“SH”) or without (“no SH”) self-healing: a) stress-strain curves. A healing rate of  $\eta=0.1$  is chosen in a distributed healing configuration. b) Normalized dissipated energy.

Clearly, the effectiveness of self-healing is greatly dependent on the mechanical properties of the “healing agent”, i.e. in biological materials, the tissue that replaces the damaged material.

This can be seen by varying the strength  $\sigma_{F_{SH}}$  of the new fibres that replace damaged ones in simulations, with respect to that of the original ones  $\sigma_{F_0}$ . Three ratios between the two strengths are considered in Fig. 6:  $\sigma_{F_0}/\sigma_{F_{SH}} = 100, 10, 1$ . Simulations show a nonlinear increase in the fatigue life  $N_C$  of the considered specimen with increasing healing rate for all three cases, but a markedly more significant maximum increase (42%) in the case of  $\sigma_{F_{SH}} = \sigma_{F_0}$ , although a significant 31% maximum increase is obtained for a poor healing agent having only  $\sigma_{F_0}/\sigma_{F_{SH}} = 100$ . This suggests the robustness of the strategy emerged in Nature during evolution of a self-healing strategy.



*Figure 6: Evaluation of the increase in fatigue life ( $N_C$ ) as a function of healing rate  $\eta$  for varying “healing agent” mechanical strength  $\sigma_{F_{SH}}$  with respect to the original material strength  $\sigma_{F_0}$ . The small differences in fatigue life imposed by huge variations of healing agent strengths suggest the self-healing robustness of the strategy emerged in Nature during evolution.*

These calculations can be used to interpret data in the literature regarding in vitro tests on biological tissue, where mechanical properties are derived without the effect of self-healing. For example, Schechtman and Bader<sup>20</sup> performed mechanical tests on human Extensor Digitorum Longus (EDL) tendons, which are involved in joint movement at the foot and ankle. In particular, they derived the fatigue life for 90 specimens as a function of the maximum fatigue stress, expressed as a percentage of the experimentally measured tendon fracture stress. This data is reported in Fig. 7 (“no SH” fitted with our model for  $\eta=0$ ), together with the corresponding fatigue life extrapolations for different values of healing rate  $\eta$ , which in this case would also be dependent on fatigue cycle speed. For example, in the case of  $\eta = 0.2$ , when cycling at 20% of the failure stress one would obtain an increase in  $N_C$  of approximately 30%. In practical terms, for an athlete this would mean that in the absence of tendon self-healing, and assuming an active sporting life of up to 40 years, tendon overuse problems or fracture would occur up to ten years earlier for equivalent loading.

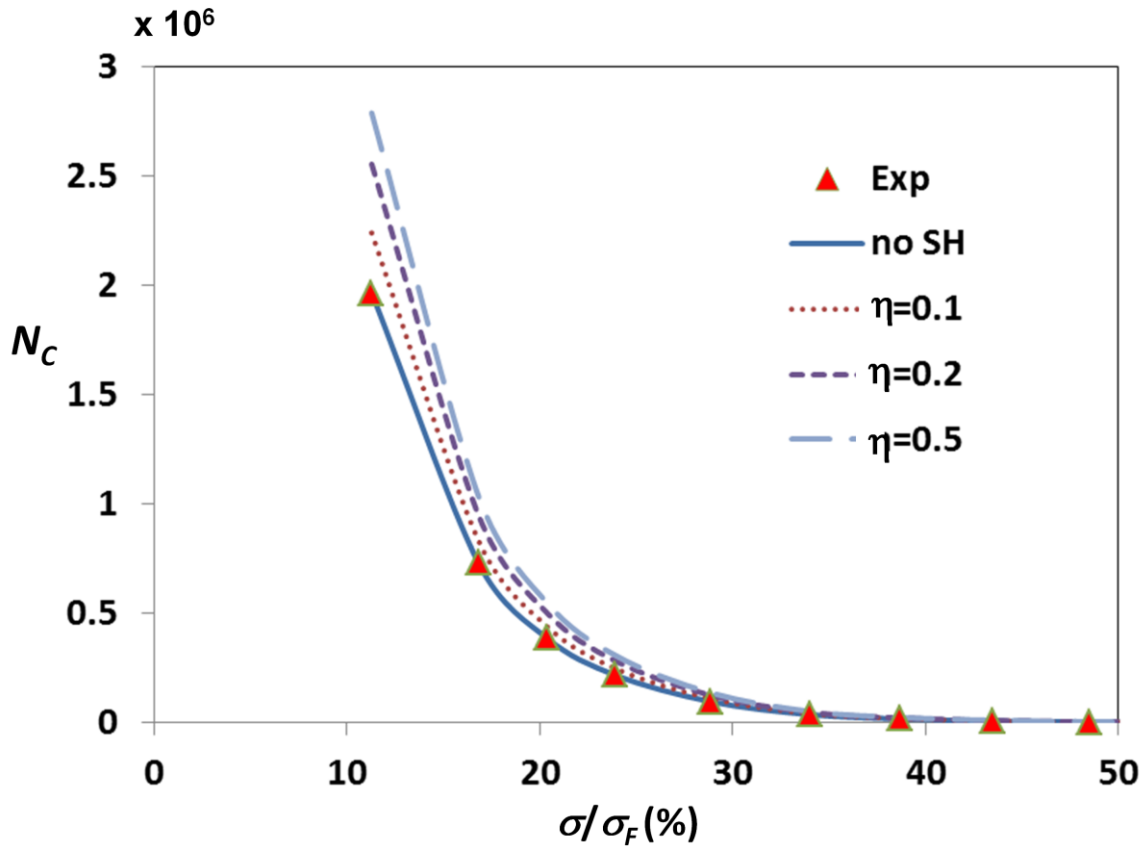


Figure 7: Fatigue life ( $N_C$ ) as a function of maximal stress amplitude divided by strength for various  $\eta$  values. Experimental data (“Exp”) fitted by the  $\eta = 0$  curve (“no SH”) are taken from<sup>20</sup>.

Simulations also allow us to verify the validity of the generalized Paris’ law hypothesised in Section 2. Results are shown in Fig.8: the scaling of fatigue life  $N_C$  of self-healing specimens with respect to  $(1-\eta)$  is calculated numerically and analytically, using Eq.6, for various initial crack lengths  $a$ , normalized with respect to the specimen width  $w$ . A saw tooth loading function is employed and the fatigue stress level is chosen to be approximately 5% of the fracture strength of fibres, so as to obtain a significant number of cycles to failure ( $>10000$ ). Numerical results show a power-law decrease in the average fatigue life with  $(1-\eta)$ ,

consistently with the theory. These can be fitted with power-law functions, as shown in the figure. Contrary to uniaxial tension numerical simulations, where localized healing proved to be considerably more effective than distributed healing in increasing fracture strength, in the case of the present fatigue simulations, the difference between results for the fatigue life in the two cases is negligible, again suggesting the robustness of the self-healing.

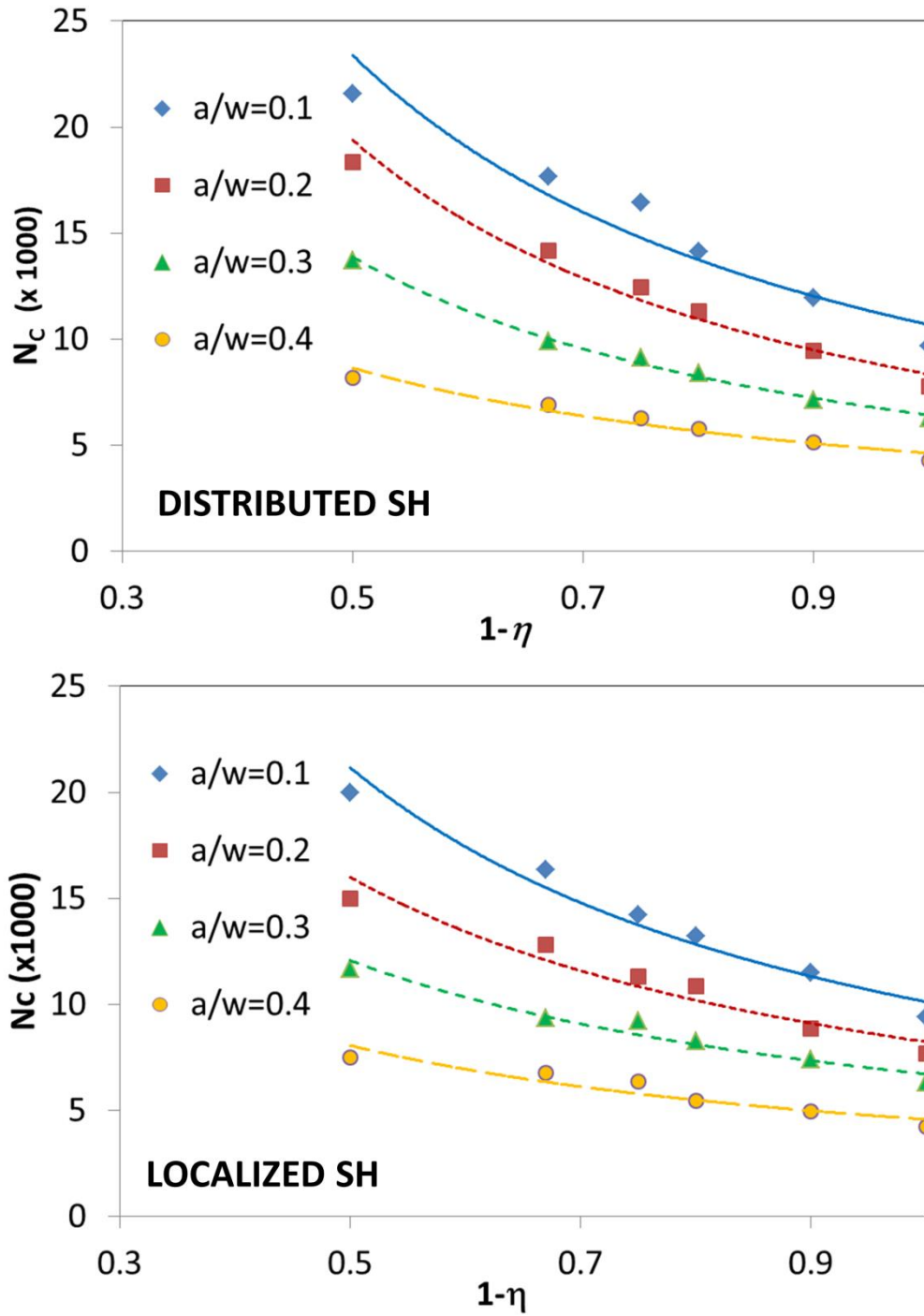


Figure 8: Dependence of numerically calculated fatigue life as a function of  $(1-\eta)$  for distributed (above) or localized (below) healing. Data are interpolated with power law curves.

To fully verify Eq. (6),  $N_C$  results are plotted versus  $a(1-\eta)$ . Figure 9 shows data for distributed healing. The numerical data can be adequately fitted using a power-law  $y=a\cdot x^b$ , with a resulting exponent of  $b=-0.698$ . Comparing this to Eq. (6) and using the previously derived value of  $\alpha = 0.7$ , we obtain a Paris exponent  $m \approx 3$ , which is in the lower range of the values found for other types of materials (mainly metals) in the literature<sup>31</sup>, which is usually indicative of extensive crack-tip plasticity in fatigue damage mechanisms. More importantly, we also notice that this  $m$  value is consistent with that used in simulations to describe the fatigue stress decrease according to Eq. (9).

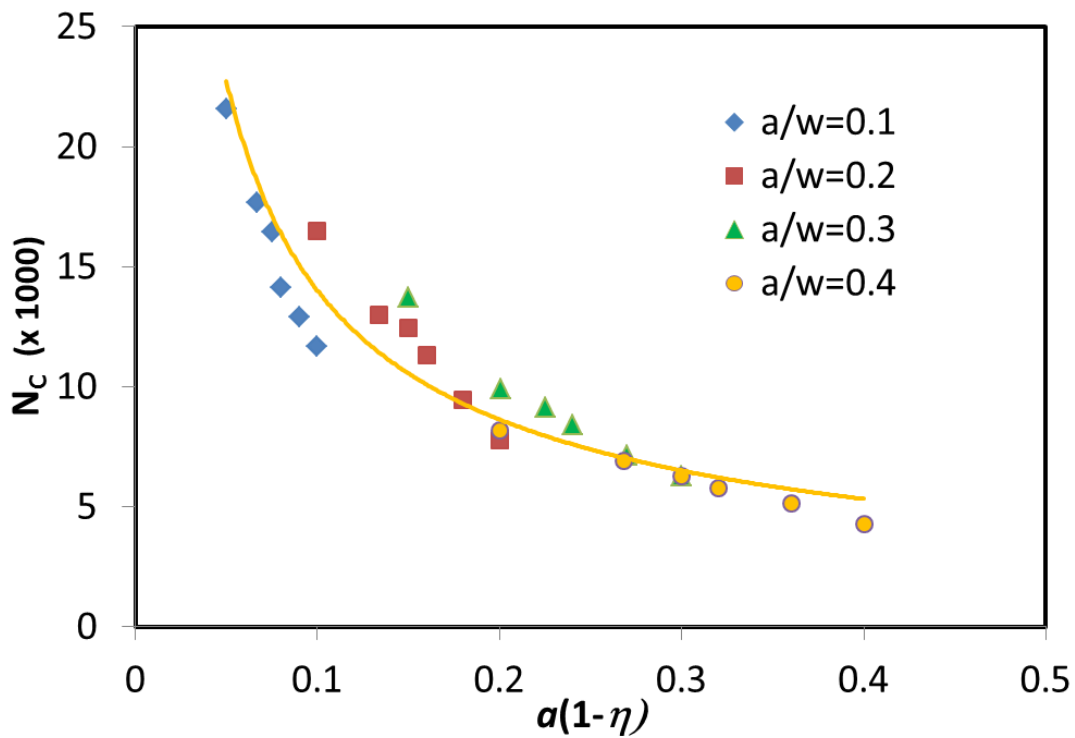


Figure 9: Numerical validation of the generalized Paris' law for self-healing materials: comparison between numerically and analytically calculated fatigue life as a function of  $a(1-\eta)$ .



## 5. Conclusions

We have developed and modified our previous code, the Hierarchical Fibre Bundle Model, to simulate fatigue damage evolution in self-healing soft nanomaterials. The model is essentially dependent on a single parameter, the material healing rate, which defines the degree of material reparation vs. material damage. How the healing occurs, whether at the location of the main advancing crack, or at random damaged locations in the specimen, does not seem to appear to influence significantly the effectiveness of the reparation process. Results show that fatigue life can be considerably improved with respect to non-self-healing specimens, with increases of up to 40% for healing rates close to 0.5. The mechanical properties of the healing agent are also shown to play a significant role: biological materials, even when the healing agent does not have similar properties to the original one, have a potential advantage over non-self-healing materials suggesting that also artificial self-healing materials, where healing agents often have reduced mechanical properties, could represent interesting bio-inspired solutions. Finally, numerical simulations are used to confirm simple scalings that have been introduced for the expressions of fracture or fatigue in the case of self-healing materials.

On the one hand, this study highlights the robustness of the self-healing strategy adopted in Nature as a consequence of evolution. On the other hand, the present numerical approach and modified analytical expressions for Paris' law provide the possibility of improving fatigue life predictions in medicine, e.g. the fatigue life of *in vivo* tendons of sportsmen. Of course, further studies are needed to verify the applicability of Paris' law, which was first developed for materials such as metals, in the field of soft materials such as tendons. However, in support of this approach, a number of studies are present in the literature for collagen-based materials (see <sup>32</sup> and references therein), particularly in the case of bone, showing that Paris' law is applicable. This, together with the particularly robust and wide-

ranging applicability of Paris' law for many materials, leads to the assumption that it should be appropriate for tendons and ligaments.

In future, the influence of hierarchy in fatigue performance will be studied in depth, and this model will also be used to develop strategies for the simultaneous optimization of multiple material properties, such as strength, toughness and fatigue life, with the objective of better understanding biological materials and thus helping in finding ultimate solutions in sport medicine, as well as in the design of novel bio-inspired materials.

**Acknowledgements:**

NMP acknowledges support from the European Research Council, ERC Ideas Starting grant n. 279985 "BIHSNAM", from ERC Proof of Concept grants n. 619448 "REPLICA2" and n. 632277 "KNOTOUGH", from the Graphene FET Flagship ("Graphene-Based Revolutions in ICT And Beyond"- Grant agreement no: 604391), and from the Autonomous Province of Trento (Graphene PAT WP10, code 81017). FB acknowledges support from BIHSNAM.

## References

1. M.A. Meyers, P.-Y. Chen, A.Y.-M. Lin and Y. Seki: Biological materials: Structure and mechanical properties *Progress in Materials Science*. **53**(1), 1 (2008).
2. B.A. Winkelstein: Orthopaedic biomechanics (CRC Press, City, 2013).
3. M.A. Meyers, J. McKittrick and P.-Y. Chen: Structural Biological Materials: Critical Mechanics-Materials Connections *Science*. **339**(6121), 773 (2013).
4. S.R. White, N.R. Sottos, P.H. Geubelle, J.S. Moore, M.R. Kessler, S.R. Sriram, E.N. Brown and S. Viswanathan: Autonomic healing of polymer composites *Nature*. **409**(6822), 794 (2001).
5. V. Sahni, J. Harris, T.A. Blackledge and A. Dhinojwala: Cobweb-weaving spiders produce different attachment discs for locomotion and prey capture *Nat Commun*. **3**, 1106 (2012).
6. K.S. Toohey, N.R. Sottos, J.A. Lewis, J.S. Moore and S.R. White: Self-healing materials with microvascular networks *Nature Materials*. **6**(8), 581 (2007).
7. C.J. Hansen, W. Wu, K.S. Toohey, N.R. Sottos, S.R. White and J.A. Lewis: Self-Healing Materials with Interpenetrating Microvascular Networks *Advanced Materials*. **21**(41), 4143 (2009).
8. E.N. Brown, S.R. White and N.R. Sottos: Retardation and repair of fatigue cracks in a microcapsule toughened epoxy composite - Part II: In situ self-healing *Composites Science and Technology*. **65**(15-16), 2474 (2005).
9. P. Cordier, F. Tournilhac, C. Soulie-Ziakovic and L. Leibler: Self-healing and thermoreversible rubber from supramolecular assembly *Nature*. **451**(7181), 977 (2008).

10. E.N. Brown, S.R. White and N.R. Sottos: Retardation and repair of fatigue cracks in a microcapsule toughened epoxy composite – Part I: Manual infiltration *Composites Science and Technology*. **65**(15–16), 2466 (2005).
11. E.N. Brown, S.R. White and N.R. Sottos: Retardation and repair of fatigue cracks in a microcapsule toughened epoxy composite—Part II: In situ self-healing *Composites Science and Technology*. **65**(15–16), 2474 (2005).
12. A.S. Jones, J.D. Rule, J.S. Moore, N.R. Sottos and S.R. White: Life extension of self-healing polymers with rapidly growing fatigue cracks *Journal of The Royal Society Interface*. **4**(13), 395 (2007).
13. E.B. Murphy and F. Wudl: The world of smart healable materials *Progress in Polymer Science*. **35**(1-2), 223 (2010).
14. A.C. BaLazs: Modelling self-healing materials *Materials Today*. **10**(9), 18 (2007).
15. A. Gautieri, S. Vesentini, A. Redaelli and M.J. Buehler: Hierarchical Structure and Nanomechanics of Collagen Microfibrils from the Atomistic Scale Up *Nano Letters*. **11**(2), 757 (2011).
16. S. Pradhan, A. Hansen and B.K. Chakrabarti: Failure processes in elastic fiber bundles *Rev Mod Phys*. **82**(1), 499 (2010).
17. N.M. Pugno, F. Bosia and A. Carpinteri: Multiscale stochastic simulations for tensile testing of nanotube-based macroscopic cables *Small*. **4**(8), 1044 (2008).
18. F. Bosia, T. Abdalrahman and N.M. Pugno: Investigating the role of hierarchy on the strength of composite materials: evidence of a crucial synergy between hierarchy and material mixing *Nanoscale*. **4**(4), 1200 (2012).
19. F. Bosia, T. Abdalrahman and N.M. Pugno: Self-Healing of Hierarchical Materials *Langmuir*. **30**(4), 1123 (2014).

20. H. Schechtman and D.L. Bader: In vitro fatigue of human tendons *J Biomech.* **30**(8), 829 (1997).
21. H. Schechtman and D.L. Bader: Fatigue damage of human tendons *J Biomech.* **35**(3), 347 (2002).
22. T.A.L. Wren, S.A. Yerby, G.S. Beaupré and D.R. Carter: Mechanical properties of the human achilles tendon *Clinical Biomechanics.* **16**(3), 245 (2001).
23. T.L. Anderson: Fracture mechanics : fundamentals and applications, 3rd ed. (Taylor & Francis, City, 2005).
24. N. Pugno, A. Carpinteri, M. Ippolito, A. Mattoni and L. Colombo: Atomistic fracture: QFM vs. MD *Engineering Fracture Mechanics.* **75**(7), 1794 (2008).
25. M.G. P.C. Paris, W.E. Anderson: A rational analytic theory of fatigue *Trend Engineering.* **13**, 9 (1961).
26. N. Pugno, P. Cornetti and A. Carpinteri: New unified laws in fatigue: From the Wohler's to the Paris' regime *Engineering Fracture Mechanics.* **74**(4), 595 (2007).
27. R. Lakes: Materials with Structural Hierarchy *Nature.* **361**(6412), 511 (1993).
28. P. Fratzl and R. Weinkamer: Nature's hierarchical materials *Progress in Materials Science.* **52**(8), 1263 (2007).
29. W. Weibull: A Statistical Theory Of The Strength Of Materials *Ingeniörsvetenskapsakademiens Handlingar.* **151**, (1939).
30. <http://www.dauin-hpc.polito.it>
31. R.O. Ritchie: Incomplete self-similarity and fatigue-crack growth *International Journal of Fracture.* **132**(3), 197 (2005).
32. P. Fratzl: Collagen: Structure and Mechanics (Springer, 2008).